



HAL
open science

Numerical features of cavitation models based on the simplified Rayleigh-Plesset equation

Catherine Ramirez, Alban Leroyer, Emmanuel Guilmineau, Patrick Queutey

► **To cite this version:**

Catherine Ramirez, Alban Leroyer, Emmanuel Guilmineau, Patrick Queutey. Numerical features of cavitation models based on the simplified Rayleigh-Plesset equation. 19th Numerical Towing Tank Symposium - NuTTS 2016, Sep 2016, St. Pierre d'Oléron, France. hal-02569359

HAL Id: hal-02569359

<https://hal.science/hal-02569359>

Submitted on 22 Jun 2020

HAL is a multi-disciplinary open access archive for the deposit and dissemination of scientific research documents, whether they are published or not. The documents may come from teaching and research institutions in France or abroad, or from public or private research centers.

L'archive ouverte pluridisciplinaire **HAL**, est destinée au dépôt et à la diffusion de documents scientifiques de niveau recherche, publiés ou non, émanant des établissements d'enseignement et de recherche français ou étrangers, des laboratoires publics ou privés.

Numerical features of cavitation models based on the simplified Rayleigh-Plesset equation

Catherine Ramirez, Alban Leroyer, Emmanuel Guilmineau, Patrick Queutey
LHEEA, UMR-CNRS 6598, Ecole Centrale Nantes
lcramire@ec-nantes.fr

1 Introduction

To reproduce and investigate cavitation phenomena, several numerical models have been developed and implemented in Computation Fluid Dynamics (CFD) solvers in the last two decades. From those models, a large number uses calibration coefficients that are mainly empirical, and even though they are set for a large set of conditions, coefficients are mostly undesirable due to the work it implies to find proper values. In this work, we propose to investigate the model of [Sauer, 2000], based on a simplified Rayleigh-Plesset equation, because it does not use coefficients. Nonetheless, it was found that the ISIS-CFD implementation of this model presents a problematic feature. Under some physical configurations, Sauer’s model exhibits a short cavitation pocket with a minimum pressure much lower than the vapor pressure, which additionally is not predicted by the experimental results neither by the models of [Merkle et al., 1998] and [Kunz et al., 2000].

Although it is not largely commented, this issue can also be depicted by some other models besides the Sauer’s one, either because of a lack of physics in the model or due to wrong numerical parameters. For instance, in the case of a foil, [Bauer and Abdel-Maksoud, 2001] show that a model based on a potential method is unable to reproduce experimental data and the results of a more sophisticated model. Or, as it is shown by [Yakubov et al., 2015], a model may present a loss in accuracy depending on the calibration coefficients used. Furthermore, it has been seen that this phenomena can be a real physical condition, as it is the case for injection nozzles due to the liquid tension, work presented by [Martynov et al., 2006]. Within this work, the studied models were compared and different mechanisms were proposed and tested in order to improve the implementation of the Sauer’s model. It was found that a modification in the Rayleigh-Plesset model exhibited good results, and additionally it was proved that there is a direct influence of the source term on the pressure response.

2 Numerical simulation of cavitation

Among the different cavitation models, two main approaches can be recognized: the heterogeneous approach and the homogeneous equilibrium. The present study is focused on models within the framework of the second approach. This approach defines a single fluid model for both phases and interaction between them is taken into account by means of a barotropic state law or by solving an advection equation for the liquid or vapor fraction, with a source term modeling the vaporization/condensation process. In this approach, density and viscosity are computed as a weighted average of the volume fraction of the two phases. The governing equations of the multiphase flow will then include, conservation of mass and momentum, and a transport equation for the cell fraction of one of the phases, as the one shown below:

$$\frac{\partial}{\partial t}(\alpha_v \rho_v) + \frac{\partial}{\partial x_i}(\alpha_v \rho_v u_i) = S. \quad (1)$$

In this equation the source term can be understood as composed by two terms as $S = \dot{m}^{vap} + \dot{m}^{cond}$, each term related to the active process, i.e. \dot{m}^{vap} stands for the vaporization process and \dot{m}^{cond} for the condensation one. As shall be seen later, the source term S is formulated mainly as a function of the pressure and the fraction of a donor phase. The advection equation (1) can be seen as a continuity equation, where the vapor fraction α_v defines the ratio of the vapor volume within the cell volume.

In this work, the solution strategy for the advection equation of the vapor fraction (1) and the turbulence model are common for all the studied models, and the cavitation models are distinct from each other only by the definition of the source term S . In that regard, turbulence effects on the cavitation process are

included through the use of the shear stress transport (SST) turbulence model of [Menter et al., 2003], and the dynamic of the mixture is predicted using a standard mono-fluid multiphase method, which is in turn related to a given mass transfer model allowing the evolution between the phases.

3 Rayleigh-Plesset equation based models

This section presents a brief description of some homogenized models that use the Rayleigh-Plesset equation as a closure for the motion equations. These models assume that micro-bubbles or cavitation nuclei n_0 exist in the liquid and are carried by it during the motion. When the liquid pressure is lowered below the vapor pressure those cavitation nuclei expand generating regions of vapor. Particularly, in a hydrofoil, the pressure decreases along the suction side, inducing the process of vaporization in the low pressure regions (near the leading edge), and the breakage of the vapor pocket downstream where the pressure recovers. Even though the model of interest is the model of Sauer, the models of Kubota and Zwart are also presented since they are useful to highlight some features of Sauer's one.

The table 1 presents an overview of the models. It shows, for each of the models, the definitions for the nuclei density n_0 , the vapor fraction α_v and the mass transfer between the phases, expressed either by the particular term according to the active process, \dot{m}_v^{vap} or \dot{m}_v^{cond} , or by the general source term S .

Table 1: Synopsis of some Rayleigh-Plesset equation based models

	Kubota et al., 1992	Zwart et al., 2004	Schnerr and Sauer, 2001
n_0	N_B/V		N_B/V_L
α_v	$V_B n_0 = \frac{4}{3}\pi R_B^3 n_0$		$\frac{V_v}{V} = \frac{n_0 4/3\pi R^3}{1 + n_0 4/3\pi R^3}$
\dot{m}_v^{vap}	$C_{vap} \frac{3\alpha_v \rho_v}{R_B} \dot{R}$	$C_{vap} \frac{3\alpha_{nuc}(1 - \alpha_v)\rho_v}{R_B} \dot{R}$	$3 \frac{\rho_l}{\rho} (1 - \alpha_v) \alpha_v \frac{\dot{R}}{R}$
\dot{m}_v^{cond}	$C_{cond} \frac{3\alpha_v \rho_v}{R_B} \dot{R}$	$C_{cond} \frac{3\alpha_v \rho_v}{R_B} \dot{R}$	$3 \frac{\rho_l}{\rho} (1 - \alpha_v) \alpha_v \frac{\dot{R}}{R}$
\dot{R}	$\sqrt{\frac{2}{3} \frac{P_R - P_\infty}{\rho_l}} = \text{sgn}(P_v - P_c) \sqrt{\frac{2}{3} \frac{ P_v - P_c }{\rho_l}}$		

Furthermore, the last line of the table presents the simplified Rayleigh-Plesset equation \dot{R} , which seeks to characterize the size evolution of a single bubble due to the change in the local pressure. This formulation assumes that bubble-bubble interactions and bubble coalescence can be neglected, and also that bubbles remain spherical all along their life. In this equation P_R is the liquid pressure at the bubble boundary, P_∞ is the one in the far field and ρ_l the density of the domain surrounding the bubble. However, in practice, P_R and P_∞ are taken as saturation vapor pressure P_v and cell pressure P_c , respectively. The models under studying additionally neglect the liquid viscosity the surface tension and the second order terms within the original equation.

One of the first models to predict cavitation by means of a multiphase mixture model based on a transport equation is the one of [Kubota et al., 1992]. This model proposes a pseudo-density calculation for the mixture and determines the volume vapor fraction using a constant nuclei density n_0 , a fixed radius R_B per unit volume and the Rayleigh-Plesset model. However, some issues are present at low void fractions for this model, which is why the model of [Zwart et al., 2004] proposes to replace the term α_v , present in \dot{m}_v^+ , by $\alpha_{nuc}(1 - \alpha_v)$. Change that allows overcoming the issue by considering that as the vapor volume fraction increases, the nucleation site density decrease accordingly. Within this model, α_{nuc} is the nucleation site volume fraction and likewise R_B is the radius of a nucleation site.

On the other hand, conversely to the models of Kubota and Zwart, [Schnerr and Sauer, 2001] propose a particular definition of the nuclei density that leads with a different expression of the source term. This model similarly adopts a constant nuclei density n_0 and bubble radius R_0 to describe the liquid quality,

nonetheless in the definition of the nuclei density, the number of bubbles is explicitly linked to the liquid volume and not to the mixture one. By doing this, the conservation of the defined quality of the liquid is guaranteed along the cavitation process. That is to say that, if the nuclei grow the vapor fraction rises and hence the water fraction decreases, and so does the number of bubbles in the cell, argument that is in accordance with the one of Zwart to improve Kubota's model.

4 Extended model of Sauer

This section presents a mechanism that was found to improve the prediction of Sauer's model, increasing the pressure so that it remains within the physical limit, and at the same time extending the cavity pocket. In order to introduce the mechanism the following analysis is done. If a homogeneous nuclei distribution is considered, for low vapor fraction values the assumption of non-interaction and non-coalescence might be correct since the bubbles contained in the computational cell would be small enough and might not be interacting with each other. Therefore, in this case, it is correct to use the liquid density to characterize the domain in which a single bubble evolves, as it stated by the Rayleigh-Plesset model. Nonetheless, when bubbles grow and the vapor fraction of a cell increases, a bubble is not anymore evolving in a purely liquid medium, which is why this work proposes to use the cell density (mixture density), instead of the pure liquid one, to characterize the surrounding domain of a bubble evolving. In this way, the initial assumption is met and the physical sense within the model is extended for high values of the vapor fraction.

Additionally, to compute the cell density instead of using an arithmetic mean, between liquid and vapor density, a modified mean was used. A function between and arithmetic and a generalized mean (with exponent $p = 0.1$) was finally implemented. Figure 3 shows that the density of the cell will be almost considered as the vapor density for vapor fractions below 0.5, it means $\rho_{cell} = \rho_v$ for $0 < \alpha_v \approx 0.5$.

Despite an extensive revision of [Sauer, 2000] aspects of the model, such as use of dynamic bubble radius or the assumption regarding the vapor density, remained unclear and were thus studied within this work. Regarding the bubble radius, it was questioned whether to fix it along the computation to the value R_0 , which corresponds to the liquid quality defined, or to compute and use an actualized radius at each iteration using the current value of the vapor fraction, as defined by the expression of the radius R in section 3. Even though the effect of a fixed radius was studied, the results are not presented here, instead, the radius R is computed at each iteration according to the original implementation of Sauer's model in the ISIS-CFD solver. Under this assumption, the model of Sauer should depict not only the mechanism of the inception, but the growing of the bubbles and the inverse process. Additionally the vapor density is neglected in the formulation of the source term.

5 Influence of the source term on the balance of the system

As mentioned before, transient effects given by the mass transfer between phases are taken into account by considering a source term in both, the VOF transport equation (1) and the pressure-equation. Using an algorithm (SIMPLE-type), this section illustrates the influence of the sign and magnitude of the source term on the pressure field. Given the algorithm used determine and couple the pressure and velocity fields for incompressible flows, using the Navier-Stokes equations, as:

$$\begin{array}{ll} \text{Prediction of the velocity} & (E - A)U^k + Gp^{k-1} = f, \\ \text{Prediction of the pressure} & DE^{-1}Gp^k = DU^{*k}, \\ \text{with} & U^{*k} = E^{-1}(AU^k + f), \\ \text{Correction of velocity} & U = U^{*k} - E^{-1}Gp^k. \end{array}$$

Applying the divergence operator on the velocity correction equation and assuming the E matrix to be diagonal, yields the relation $DE^{-1}Gp = DU^* - DU$. There, the terms DU and DU^* are considered to be source of change for the pressure, and the behavior of the left hand side term is assimilated as proportional to the Laplacian of the pressure, i.e. $DE^{-1}Gp \approx \beta\Delta p$.

It is recalled that for a non-cavitating flow, the continuity equation yields $\nabla \vec{u} = 0$. However, when cavitation is presented, the source term on the continuity equation (1) is active and $\nabla \vec{u}$ is no longer zero,

instead the expression $\nabla \vec{u} = \frac{\rho_l - \rho_v}{\rho_v \rho_l} S$ yields. Under cavitation condition, the term DU can be directly linked to the cavitation and DU^* to the changes in the velocity. Furthermore, the resultant pressure can be determined by the linear contribution of two sources, one related to the cavitation (Δp^c) and other to the change in velocities (Δp^v), as noted below:

$$\begin{aligned} \beta \Delta p &\approx \underbrace{\beta \Delta p^v}_{\text{velocity Src}} + \underbrace{\beta \Delta p^c}_{-\text{cavitation Src.}} \\ \beta \Delta p &\approx \text{velocity Src} + -\text{cavitation Src.} \end{aligned} \quad (2)$$

Finally, if it is considered that $\rho_v \ll \rho_l$, it is possible say that $\Delta \vec{u} \approx \dot{m}_v$, and therefore a simplified relation between the pressure evolution and the source term can be expressed as $\Delta p^c \approx -\dot{m}_v/\beta$.

5.1 1D Analytical example

To study the influence of the source term on the pressure, the following set of two 1D polynomial equations is proposed. It consists of an analogical term for the cavitation source $\dot{f}(x)$ and the resultant analog pressure obtained after double integration $f(x)$, for the process of vaporization and condensation.

$$\begin{aligned} \dot{f}(x)^{vap} &= x(1-x), (\dot{m}_v^{vap}) & \dot{f}(x)^{cond} &= x(x-1), (\dot{m}_v^{cond}) \\ -f(x)^{vap} &= -(x^4/12 - x^3/6 + x/12), (p^{c^{vap}}) & -f(x)^{cond} &= -(x^3/6 - x^4/12 - x/12), (p^{c^{cond}}) \end{aligned}$$

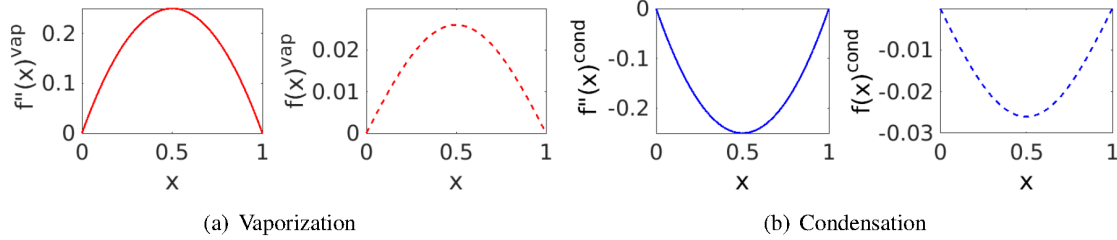


Fig. 1: Analog expression of the source term $\dot{f}(x)$ and the response, or analog expression of the pressure, $f(x)$.

It is highlighted here that the sign obtained for the function $f(x)$ is changed after the integration in order to consider the negative sign shown in equation (2), and directly see the effect of the source term. As it is shown in the Figure 1, it can be stated that a positive source term \dot{m}_v^+ , as is the case during the vaporization process, will tend to increase the resultant pressure, while a negative one will lead with an decrease it. This correlation explains how this mechanism leads to a stabilization of the pressure inside the cavity pocket, as shown in Figure 2.

6 Simulation setup

For the present study a 2D steady cavitating flow over an hydrofoil NACA66(MOD) is considered. The hydrofoil is described by a camber ratio of $Y_c/C = 0.020$, a NACA mean line of $a = 0.8$ and a thickness ratio of $t/C = 0.09$, where t is the maximum thickness, Y_c the maximum camber and C the chord length of the hydrofoil section. The hydrofoil model was considered completely smooth and with the chord length $C = 0.15\text{m}$. The main analysis is performed with a free-stream velocity of $U = 12\text{m/s}$, a cavitation fraction of $\sigma = 1$ and angle of attack $\alpha = 4^\circ$, although simulations using $\sigma = 0.91$ and $\sigma = 0.84$ are also performed. The fluid kinematic viscosity is set to $\nu = 8.92 \times 10^{-7}\text{m}^2/\text{s}$ and liquid and vapor density are kept constant and equal to $\rho_l = 997\text{kg/m}^3$ and $\rho_v = 0.02308\text{kg/m}^3$, respectively. A mesh of 59874 elements with a turbulence wall-resolved approach ($y^+ = 1$) is used. The experimental results described in [Shen and Dimotakis, 1989] are taken as a reference.

7 Results and conclusion

To sketch the statement described in section 5, Figure 2 shows the resultant profile of the normalized pressure coefficient, for the test case, with the cavitation module enabled and disable during the simulation. Figure 2(a) shows that along the upper face of the profile the pressure reach values below the vapor pressure making evident the formation of vapor. Figure 2(b) presents the resultant C_p when the

cavitation module is enabled, it shows that the pressure on the upper surface does not go below the vapor pressure and instead a flat region around the saturation vapor pressure value, corresponding to the cavitation pocket, is formed.

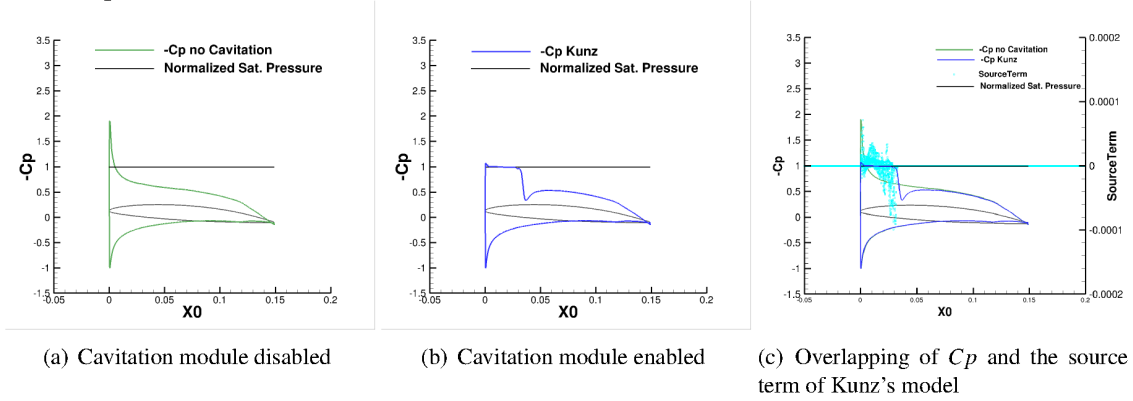


Fig. 2: Normalized pressure coefficient C_p around a hydrofoil (test case).

Figure 2(c) summarizes the process, overlaying the two previous graphs with the resultant source term of Kunz's model. It can be confirmed that in regions where pressure tends to go below the vapor pressure, the source term acts on the pressure equation in such a way that the pressure will be increased, and on the contrary the source term reduces the pressure on the region where the pressure is above the vapor pressure, keeping the pressure around the value of vapor pressure along the sheet cavitation.

Regarding the results of the mechanism proposed, Figure 3 presents the modified mean used to model the mixture density implemented, as it was described in section 4. Figure 4 presents the comparison between the original implementation of Sauer's model and the extended version proposed in this work. Using the barotropic law of Delannoy (similarly to what is done in [Frikha et al., 2008]), the liquid mass transfer \dot{m}_l for a given vapor fraction α_v is plot. It is remarked that the use of the mixture density increments the magnitude of the source term for low values of the vapor fraction.

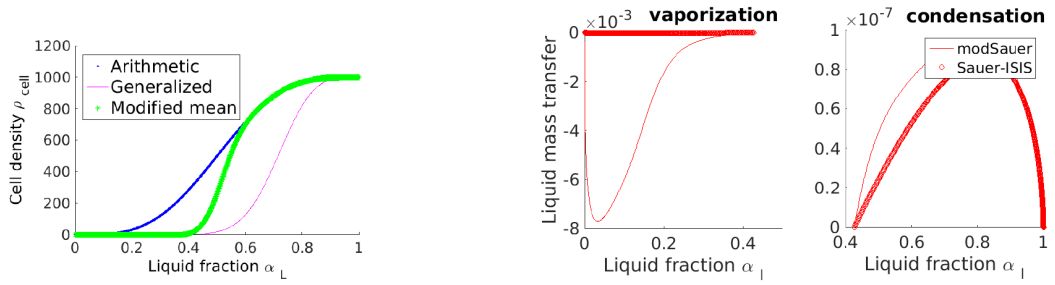


Fig. 3: Different studied means of the cell density. Fig. 4: Not normalized $\dot{m}_l^{vap}(\alpha_l)$ and $\dot{m}_l^{cond}(\alpha_l)$.

Furthermore, to illustrate the improvement achieved by the modification proposed, Figure 5 presents the resultant normalized pressure coefficient $-C_p$ along the foil surface of the test case, for the ISIS implemented models, and Figure 6 presents the results for the original and the extended implementation of Sauer's model. The pressure predicted by the original model of Sauer is extremely low compared with the one determined by the other models and the one depicted by the experimental results. Nonetheless, the modified version of Sauer leads with a prediction closer to the experimental results, not only reducing the peak of low pressure, but also increasing the length of the sheet cavitation.

Within this work it has been shown that given the influence on the pressure equation, the defect of Sauer's model could be related with the magnitude of the mass transfer term. Keeping this in mind, the source term was increased, for the range of low vapor fraction, using a physical concept within the simplified Rayleigh equation, which leads with the improvement of the prediction of cavitation phenomena done by this model.

Unfortunately, when studying the modified model of Sauer, it was observed a large dependency to the turbulence modeling approach. That is to say that good results are obtained when using a wall-resolved turbulence model for the boundary layer, however they are lost when a wall function is used, and moreover. This issue may be caused by the larger velocity imposed, near the foil, when a wall function is used, which rapidly convects the short vapor induced by the source term. Therefore, for Sauer's model, the process of vaporization has to deal, first, with the low magnitude of the source term, but also with the fact that this term will be quickly convected. On the contrary, this dependency is less observed for the other cavitation models. They overcome the lack of physics, imposed with the use of the wall-function approach, with a source term larger, by several orders of magnitude.

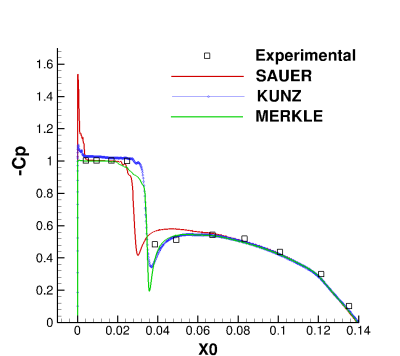


Fig. 5: $-Cp$ ISIS-CFD models

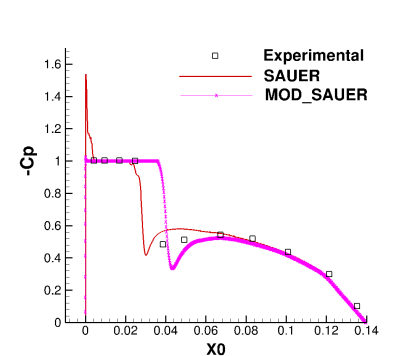


Fig. 6: $-Cp$ Original and Extended Sauer

The improvement of the model is still ongoing, nonetheless given the benefits of a model and the improvements achieved, this work seeks to expand the modified model of Sauer to be used with a wall function approach, and the future work include to assess the model with different foils, unsteady conditions and also 3D flow condition.

References

- Bauer, M. and Abdel-Maksoud, M. (2001). A 3-D Potential Based Boundary Element Method for Modelling and Simulation of Marine Propeller Flows. *German Research*.
- Frikha, S., Coutier-Delgosa, O., and Astolfi, J. A. (2008). Influence of the cavitation model on the simulation of cloud cavitation on 2D foil section. *International Journal of Rotating Machinery*.
- Kubota, A., Kato, H., and Yamaguchi, H. (1992). A new modelling of cavitating flows: a numerical study of unsteady cavitation on a hydrofoil section. *Journal of fluid Mechanics*, 240:59–96.
- Kunz, R. F., Boger, D. A., Stinebring, D. R., Chyczewski, T. S., Lindau, J. W., Gibeling, H. J., Venkateswaran, S., and Govindan, T. (2000). A preconditioned navier–stokes method for two-phase flows with application to cavitation prediction. *Computers & Fluids*, 29(8):849–875.
- Martynov, S., Mason, D., and Heikal, M. (2006). Numerical simulation of cavitation flows based on their hydrodynamic similarity. *International Journal of Engine Research*, 7(3):283–296.
- Menter, F., Ferreira, J. C., Esch, T., and Konno, B. (2003). The sst turbulence model with improved wall treatment for heat transfer predictions in gas turbines. In *Proceedings of the international gas turbine congress*, pages 2–7.
- Merkle, C. L., Feng, J., and Buelow, P. E. (1998). Computational modeling of the dynamics of sheet cavitation. In *3rd International symposium on cavitation, Grenoble, France*, volume 2, pages 47–54.
- Sauer, J. (2000). *Instationäre kavitierende Strömungen: ein neues Modell, basierend auf front capturing (VoF) und Blasendynamik*. PhD thesis, Karlsruhe, Univ., Diss., 2000.
- Schnerr, G. H. and Sauer, J. (2001). Physical and numerical modeling of unsteady cavitation dynamics. In *Fourth international conference on multiphase flow, New Orleans, USA*, volume 1.
- Shen, Y. and Dimotakis, P. E. (1989). The influence of surface cavitation on hydrodynamic forces. *American Towing Tank Conference.*, (22nd).
- Yakubov, S., Maquil, T., and Rung, T. (2015). Experience using pressure-based CFD methods for Euler-Euler simulations of cavitating flows. *Computers and Fluids*, 111:91–104.
- Zwart, P. J., Gerber, A. G., and Belamri, T. (2004). A Two-Phase Flow Model for Predicting Cavitation Dynamics. (152).